Clinical Research in Cardiology (2020) 109:339–349
https://doi.org/10.1007/s00392-019-01514-x

ORIGINAL PAPER

Culprit vessel-related myocardial mechanics and prognostic implications following acute myocardial infarction

Sören J. Backhaus[1,2] · Johannes T. Kowallick[2,3] · Thomas Stiermaier[4,5] · Torben Lange[1,2] · Alexander Koschalka[1,2] · Jenny-Lou Navarra[1,2] · Joachim Lotz[2,3] · Shelby Kutty[6] · Boris Bigalke[7] · Matthias Gutberlet[8] · Hans-Josef Feistritzer[9] · Gerd Hasenfuß[1,2] · Holger Thiele[9] · Andreas Schuster[1,2,10] · Ingo Eitel[4,5]

Received: 10 January 2019 / Accepted: 21 June 2019 / Published online: 5 July 2019

Abstract

Background Prognosis in acute myocardial infarction (AMI) depends on the amount of infarct-related artery (IRA)-subtended myocardium and associated damage but has not been described in great detail. Consequently, we sought to describe IRA-associated pathophysiological consequences using cardiac magnetic resonance (CMR).

Methods 1235 AMI patients ($n=795$ ST-elevation (STEMI) and 440 non-STEMI) underwent CMR following percutaneous coronary intervention. Blinded core-laboratory data were compared according to left anterior descending (LAD), left circumflex (LCx) and right coronary artery (RCA) regarding major adverse clinical events (MACE) within 12 months. Left ventricular (LV) global longitudinal/circumferential/radial (GLS/GCS/GRS) as well as left atrial (LA) total (ε_s), passive (ε_e) and active (ε_a) strains were determined using CMR-feature tracking. Tissue characterisation included infarct size (IS) and microvascular obstruction.

Results LAD and LCx were associated with higher mortality compared to RCA lesions (4.6% and 4.4% vs 1.6%). LAD lesions showed largest IS (16.8%), largest ventricular [LV ejection fraction (EF) 47.4%, GLS −13.2%, GCS −20.8%] and atrial (ε_s 20.2%) impairment. There was less impairment in LCx (IS 11.8%, LVEF 50.8%, GLS −17.4%, GCS −25.0%, ε_s 20.7%) followed by RCA lesions (IS 11.3%, LVEF 50.8%, GLS −19.1%, GCS −26.6%, ε_s 21.7%). In AUC analyses, ε_s (LAD, RCA) and GLS (LCx) best predicted MACE (AUC > 0.69). Multivariate analyses identified ε_s ($p=0.017$) in LAD and GLS ($p=0.034$) in LCx infarcts as independent predictors of MACE.

Andreas Schuster and Ingo Eitel contributed equally to this work.

Electronic supplementary material The online version of this article (https://doi.org/10.1007/s00392-019-01514-x) contains supplementary material, which is available to authorized users.

✉ Andreas Schuster
andreas_schuster@gmx.net

1 Department of Cardiology and Pneumology, University Medical Center Göttingen, Georg-August University, Göttingen, Germany

2 German Center for Cardiovascular Research (DZHK), Partner Site Göttingen, Göttingen, Germany

3 Institute for Diagnostic and Interventional Radiology, University Medical Center Göttingen, Georg-August University, Göttingen, Germany

4 Medical Clinic II (Cardiology/Angiology/Intensive Care Medicine), University Heart Center Lübeck, University Hospital Schleswig-Holstein, Lübeck, Germany

5 German Center for Cardiovascular Research (DZHK), Partner Site Hamburg/Kiel/Lübeck, Lübeck, Germany

6 Children's Hospital and Medical Center, University of Nebraska College of Medicine, Omaha, NE 68114, USA

7 Department of Cardiology, Charité Campus Benjamin Franklin, University Medical Center Berlin, Berlin, Germany

8 Institute of Diagnostic and Interventional Radiology, Heart Center Leipzig at University of Leipzig, Leipzig, Germany

9 Department of Internal Medicine/Cardiology, Heart Center Leipzig at University of Leipzig, Leipzig, Germany

10 Department of Cardiology, Royal North Shore Hospital, The Kolling Institute, Northern Clinical School, University of Sydney, 5th Floor, Acute Services Building, Reserve Road, St Leonard's, Sydney, NSW 2065, Australia

Conclusions CMR allows IRA-specific phenotyping and characterisation of morphologic and functional changes. These alterations carry infarct-specific prognostic implications, and may represent novel diagnostic and therapeutic targets following AMI.

Trial registration ClinicalTrials.gov: NCT00712101 and NCT01612312

Graphic abstract

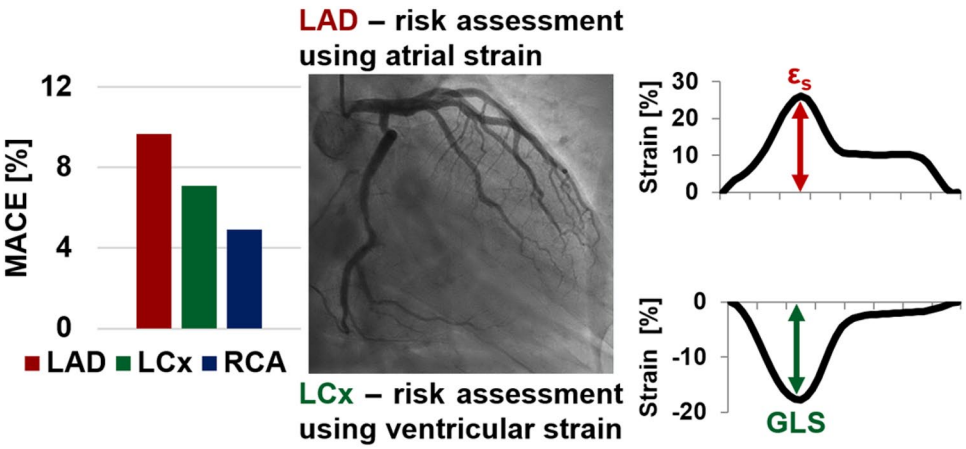

Keywords Infarct-related artery · Cardiac function · Cardiovascular magnetic resonance · Feature tracking · Prognosis

Introduction

Percutaneous coronary intervention (PCI) plays a key role in the management of acute myocardial infarction (AMI) and ischemic heart failure development [1]. Since the burden of cardiovascular disease remains high [2], optimized risk stratification and patient management following AMI are essential for effective therapy and mortality reduction [3–6]. Anterior AMI with lesions in either the left main (LM) [7–9] or left anterior descending (LAD) [10–13] is associated with increased risks for major adverse clinical events (MACE) and mortality. However, some trials also reported no infarct-related artery (IRA)-dependant differences in mortality [14, 15]. At present, the underlying pathophysiology has not extensively been described and there is evidence to suggest that sheer infarct size is not sufficient to explain differences in outcome [12]. Cardiovascular magnetic resonance (CMR) allows for adequate morphologic and functional quantitative myocardial phenotyping and represents an ideal tool to close the aforementioned evidence gap [16, 17]. Consequently, we sought to comprehensively describe pathophysiological alterations associated with specific IRA and define their relative contributions towards disease progression and outcome in a large prospective multi-center study of STEMI and NSTEMI patients [18–21].

Methods

Study population

This sub-study included patients previously enrolled in two clinical trials (AIDA STEMI, Abciximab Intracoronary versus intravenously Drug Application in STEMI, NCT00712101 [22] and TATORT NSTEMI, Thrombus Aspiration in Thrombus Containing Culprit Lesions in Non-ST-Elevation, NCT01612312 [23]) who further underwent CMR imaging following AMI treated by primary PCI. The AIDA STEMI trial randomized 2065 STEMI patients to either intracoronary ($n = 1032$) or intravenous ($n = 1033$) abciximab application (0.25 mg/kg bodyweight) during PCI and recruited 795 patients at eight study sites across Germany with expertise in CMR imaging to a CMR substudy. The TATORT NSTEMI trial prospectively recruited 440 NSTEMI patients to aspiration thrombectomy ($n = 221$) or standard PCI ($n = 219$) across seven German study sites, all of which underwent CMR imaging for the investigation of CMR infarct characteristics. The lead ethical committee at the University of Leipzig as well as all local ethical committees of involved partner sites approved the studies which were conducted according to the principles of the Helsinki Declaration. All patients gave written informed consent before randomization. The CMR sub-study was supported by the German Centre for Cardiovascular Research (DZHK).

Cardiovascular magnetic resonance imaging and deformation analyses

CMR imaging was performed on 1.5- and 3.0-Tesla scanners within the first 10 days following PCI [24]. Exclusion criteria for CMR imaging comprised the established contraindications [24, 25]. The protocol included balanced steady-state free precession (bSSFP) sequences for functional cardiac analyses, T2-weighted sequences for oedema assessment and inversion-recovery gradient-echo sequences 10–20 min after the administration of gadolinium-based contrast agents for the evaluation of myocardial salvage, infarct size (IS) and microvascular obstruction (MVO) [25]. Left ventricular ejection fraction (LVEF), as well as global circumferential (GCS) and radial strain (GRS), were evaluated in the short axis (SA) stacks, the latter at basal, midventricular and apical locations. Slice positions were predefined according to imaging standard operating procedures [26]. The apical slice was required to show end-systolic blood pool, the most basal slice should not include the outflow tract in any timeframe and the midventricular slice is chosen halfway in between in the presence of papillary muscles [27]. Global longitudinal strain (GLS) and LA strain parameters were assessed in the two and four chamber view (CV) [28, 29]. LA strain analyses comprised the three physiological functions including reservoir function (total strain εs) defined as the collection of pulmonary venous return during the ventricular systole, conduit function (passive strain εe) representing the passive ventricular filling during early diastole and booster pump function (active strain εa) responsible for active augmentation of ventricular filling during late diastole [28, 30]. Strain analyses were conducted employing CMR-FT on bSSFP images using dedicated and extensively validated offline postprocessing software (2D CPA MR, Cardiac Performance Analysis, Version 1.1.2, TomTec Imaging Systems, Unterschleissheim, Germany) in an experienced and blinded core-laboratory [31–34]. LV borders were tracked endo- and epicardially, LA borders endocardially. The borders were manually traced in end-diastole and automatically propagated throughout the cardiac cycle by the software algorithm (Fig. 1). Accuracy was visually reviewed, if necessary, manual corrections were made to the initial contour only, prior to reapplying the algorithm. Final strain values were calculated from the average of three independent measurements [26, 35].

Clinical endpoints

Clinical endpoints were predefined as occurrence of MACE within 1 year following AMI including all-cause mortality, reinfarction and readmission due to congestive heart failure. To avoid statistical interference, each patient could only account for one specific event graded in the specific order of death > reinfarction > congestive heart failure. MACE occurrence was reported by each individual study site; their relevance and classification were evaluated by a blinded committee. The exact definition of the individual endpoints is described elsewhere [22, 23].

Statistical analyses

Statistical analyses compared differences in CMR-derived infarct characteristics and cardiac mechanics in relation to the underlying IRA. IRA was classified according to LAD, LCx and the right coronary artery (RCA) lesions. Categorial variables are reported in absolute numbers with corresponding percentage values and were compared using the Chi-square or, where appropriate, Fisher exact test. Continuous variables

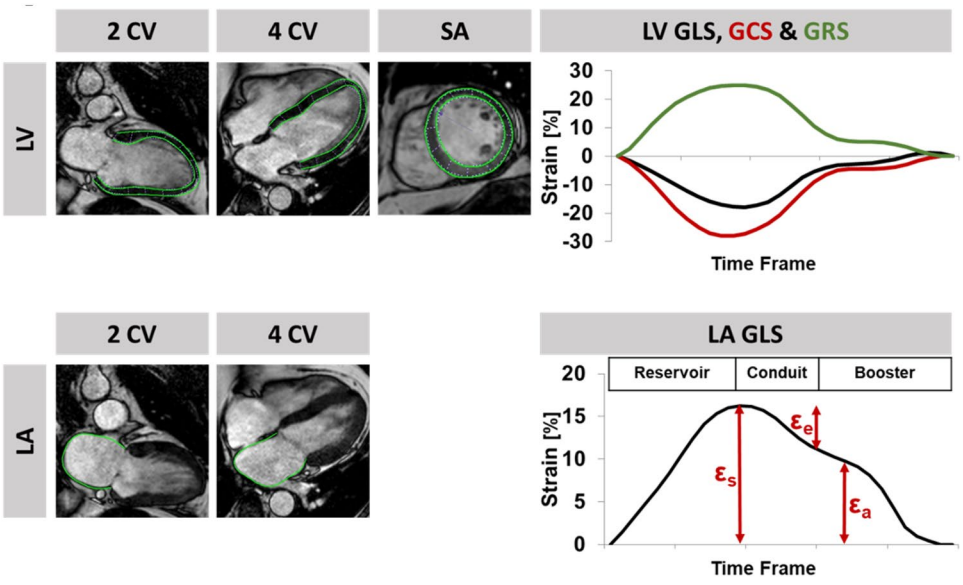

Fig. 1 Strain analyses. At the upper half, exemplary presentation of end-diastolic two and four chamber view (CV) as well as midventricular short axis (SA) views with endo- and epicardially tracked borders in the left ventricle (LV). Situated to the right, corresponding strain curves of LV global longitudinal (GLS), circumferential (GCS) and radial (GRS) strain. At the bottom half, end-systolic two and four CV of the left atrium (LA) with corresponding atrial strain curves including subsequent functional classification of reservoir (ε_s), conduit (ε_e) and booster pump (ε_a) function

were tested for normal distribution using the Shapiro–Wilk test, reported in median values with 25% and 75% interquartile range (IQR) and compared using the Mann–Whitney *U* test. Impact on MACE and mortality was evaluated using uni- and stepwise multivariate cox-regression analyses which are reported by hazard ratio (HR) with corresponding 95% confidence interval (CI) and are further complemented by area under the curve (AUC) analyses. Survival was displayed using Kaplan–Meier plots with associated Log-rank testing to determine statistical significance. All analyses were conducted using IBM SPSS Statistic Software Version 24 for Windows (IBM, Armonk, NY, USA). *p* values provided are two-sided and considered as significant below 0.05.

Results

Study population

In total, 1235 MI patients have been enrolled in the CMR sub-study and were classified according to IRA (LAD $n=498$, LCx $n=270$ and RCA $n=449$). Coronary artery bypass grafts ($n=12$) and left main coronary arteries (LCA) ($n=6$) have been excluded from statistical evaluations due to their small number. Exclusions from the study were made due to poor image quality or incomplete study protocols preventing postprocessing analyses. In total 1095 ventricular and 1035 atrial functional evaluations were incorporated into final statistical evaluations. Of these, 75 patients experienced MACE during the 1-year follow-up period (Fig. 2). CMR imaging was performed in median on day 3 (IQR 2–4) after symptom onset in all IRA subgroups. Most baseline characteristics were similar comparing different IRA subgroups and are reported in Table 1. Patients with RCA culprit lesions suffered more often from STEMI than NSTEMI (RCA 76.6%, LAD 69.7% and LCx 35.9%). Patients with LCx lesions were more frequently hypertensive and on antihypertensive medications. Treatment strategy, frequency of intervention and stent implantation, treatment success as defined by post interventional TIMI flow grade were similar between all subgroups ($p>0.05$).

Infarct characteristics and cardiac functional evaluation

Detailed CMR-derived infarct characteristics and cardiac functional parameters classified in subgroups according to IRA are reported in Table 2. In tissue characterisation, LAD lesions were associated with largest IS and area at risk ($p<0.001$ for both) and second largest MVO. LCx lesions were associated with largest MVO. RCA lesions were associated with smallest MVO and IS, the latter not significantly smaller compared to LCx lesions ($p=0.691$).

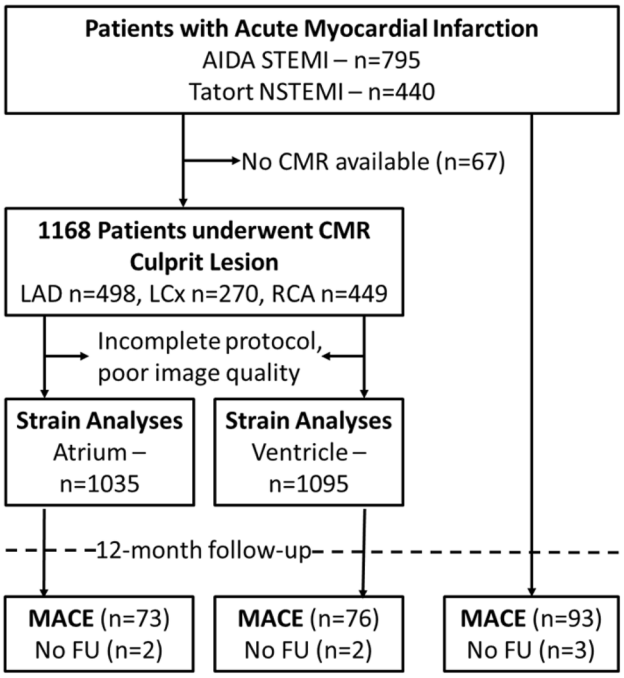

Fig. 2 Study flow chart

LV dysfunction as assessed by impaired LVEF, GLS, GCS and GRS was most pronounced for LAD followed by LCx and RCA lesions. Similarly, LA dysfunction as assessed by reservoir and conduit function was most pronounced in LAD followed by LCx and RCA lesions, but not significantly different comparing LAD and LCx lesions. There were no differences for active booster pump contractility between IRA. Subgroups of STEMI and NSTEMI are reported in the supplements, Tables S1 and S2. Differences in IRA-dependent infarct characteristics and cardiac functional parameters were distinctly less pronounced in NSTEMI compared to STEMI patients. IS was smaller in NSTEMI as compared to STEMI patients ($p<0.001$). LV GLS was the only parameter differing both in STEMI and NSTEMI patients between all IRA subgroups.

Outcome

Observed differences

MACE occurrence was numerically highest in LAD lesions (9.6%), not statistically different from LCx (7.1%, $p=0.208$) but significantly higher compared to RCA lesions (4.9%, $p=0.006$, Fig. 3a). Mortality was similar in LAD (4.6%) and LCx lesions (4.4%, $p=0.954$) and lower in RCA lesions (1.6%, LAD vs RCA $p=0.007$, LCx vs RCA $p=0.017$, Fig. 3b).

CMR-derived tissue characterisation as well as cardiac functional parameters classified according to IRA and

Table 1 Baseline characteristics

Variable	Primary lesion			*p* value		
	LAD *n* = 498	LCX *n* = 270	RCA *n* = 449	LAD vs LCx	LCx vs RCA	RCA vs LAD
Age	65 (53, 73)	66 (54, 74)	63 (52,72)	0.262	**0.013**	0.109
Sex (m)	366/498 (73.5%)	208/270 (77.0%)	336/449 (74.8%)	0.281	0.505	0.638
Cardiovascular risk factors						
Active smoking	179/459 (39.0%)	107/251 (42.6%)	204/418 (48.8%)	0.346	0.121	**0.003**
Hypertension	360/495 (72.7%)	201/269 (74.7%)	308/449 (68.6%)	0.551	0.080	0.164
Hyperlipoproteinemia	173/495 (34.9%)	107/268 (39.9%)	177/449 (39.4%)	0.173	0.968	0.126
Diabetes	117/496 (23.6%)	74/268 (27.6%)	88/449 (19.6%)	0.220	**0.013**	0.137
Body mass index (kg/m^2)	27.7 (25.3, 30.9)	27.4 (24.8, 30.2)	27.2 (24.8, 30.1)			
Previous myocardial infarction	25/498 (5.0%)	22/269 (8.2%)	34/448 (7.6%)	0.082	0.776	0.103
Previous PCI	32/498 (6.4%)	22/269 (8.2%)	47/449 (10.5%)	0.365	0.314	**0.025**
Previous CABG	6/498 (1.2%)	5/269 (1.9%)	9/449 (2.0%)	0.467	0.891	0.325
ST-segment elevation	347/498 (69.7%)	97/270 (35.9%)	344/449 (76.6%)	**< 0.001**	**< 0.001**	**0.016**
Systolic blood pressure (mmHg)	136 (120, 150)	140 (120, 153)	131 (118, 150)	0.618	**0.027**	**0.026**
Diastolic blood pressure (mmHg)	80 (71, 90)	80 (70, 90)	80 (70, 88)	0.893	**0.035**	**0.006**
Heart rate (beats/min)	78 (70, 87)	77 (69, 87)	74 (65, 85)	0.822	**0.012**	**0.001**
Time symptoms to balloon[a] (min)	190 (114, 348)	191 (113, 330)	159 (100, 285)	0.733	0.116	**0.004**
door-to-balloon time[a] (min)	29 (21, 39)	34 (24, 45)	29 (22, 44)	**0.026**	0.179	0.271
Killip class on admission						
1	422/498 (84.7%)	239/270 (88.5%)	414/449 (92.2%)	0.133	0.394	**< 0.001**
2	56/498 (11.2%)	22/270 (8.1%)	23/449 (5.1%)			
3	16/498 (3.2%)	4/270 (1.5%)	5/449 (1.1%)			
4	4/498 (0.8%)	5/270 (1.9%)	7/449 (1.6%)			
Coronary artery disease						
1	272/498 (54.6%)	120/270 (44.4%)	220/449 (49.0%)	**0.026**	0.098	**0.045**
2	144/498 (28.9%)	97/270 (35.9%)	127/449 (28.3%)			
3	82/498 (16.5%)	53/270 (19.6%)	102/449 (22.7%)			
TIMI flow grade before PCI						
0	230/498 (46.2%)	137/270 (50.7%)	242/449 (53.9%)	0.090	0.672	**0.031**
1	62/498 (12.4%)	26/270 (9.6%)	48/449 (10.7%)			
2	122/498 (24.5%)	50/270 (18.5%)	79/449 (17.6%)			
3	84/498 (16.9%)	57/270 (21.1%)	80/449 (17.8%)			
Stent implanted	484/498 (97.2%)	257/270 (95.2%)	440/449 (98.0%)	0.293	0.275	0.344
TIMI flow grade after PCI						
0	12/498 (2.4%)	5/270 (1.9%)	8/449 (1.8%)	0.926	0.992	0.790
1	10/498 (2.0%)	5/270 (1.9%)	7/449 (1.6%)			
2	41/498 (8.2%)	20/270 (7.4%)	33/449 (7.3%)			
3	435/498 (87.3%)	240/270 (88.9%)	401/449 (89.3%)			
Medication						
Glycoprotein IIb/IIIa inhibitor	355/498 (71.3%)	109/270 (40.4%)	350/449 (78.0%)	**< 0.001**	**< 0.001**	**0.019**
Aspirin	497/498 (99.8%)	267/270 (98.9%)	449/449 (100%)	0.094	**0.025**	0.342
Clopidogrel/prasugrel/Ticagrelor	498/498 (100%)	270/270 (100%)	449/449 (100%)	–	–	–
Betablocker	481/496 (97.0%)	253/270 (93.7%)	422/449 (94.0%)	**0.031**	0.878	**0.026**
ACE-inhibitor/AT-1 antagonist	467/496 (94.2%)	231/270 (85.6%)	412/449 (91.8%)	**< 0.001**	**0.009**	0.149
Aldosterone antagonist	95/496 (19.2%)	45/270 (16.7%)	25/449 (5.6%)	0.395	**< 0.001**	**< 0.001**
Statin	473/496 (95.4%)	255/270 (94.4%)	430/449 (95.8%)	0.576	0.418	0.763
Time to MRI (days)	3 (2, 4)	3 (2, 4)	3 (2, 4)	0.232	**0.035**	0.181

Data presented as *n*/*N* (%) or median (IQR). *p* values were calculated for the comparison of infarct-related arteries ($p1$ = LAD vs LCX, $p2$ = LCx vs RCA and $p3$ = RCA vs LAD), continuous variables were tested using the Mann–Whitney *U* test, categorial variables were tested using the Chi-square test of Fisher exact test as appropriate. *p* values in bold type indicate a significant difference

CABG coronary artery bypass graft, *MACE* major adverse cardiac event, *PCI* percutaneous coronary intervention, *TIMI* thrombolysis in myocardial infarction

[a]Only assessed in STEMI patients (*n* = 795)

Table 2 Cardiac performance

Parameter	Primary lesion			*p* value			
	LAD ($n=498$)	LCX ($n=270$)	RCA ($n=449$)	Overall	LAD vs LCX	LCx vs RCA	RCA vs LAD
Area at risk	34.2 (25.0, 48.7)	23.2 (18.1, 31.6)	27.6 (18.6, 39.1)	**< 0.001**	**< 0.001**	**0.002**	**< 0.001**
Infarct size	16.8 (6.80, 26.3)	11.8 (5.20, 19.2)	11.3 (5.20, 19.0)	**< 0.001**	**< 0.001**	0.691	**< 0.001**
MS index	54.1 (32.8, 74.6)	47.7 (27.9, 70.1)	58.5 (39.1, 78.9)	**0.002**	0.112	**0.001**	**0.021**
MVO	0.63 (0.00, 2.49)	1.20 (0.00, 3.20)	0.00 (0.00, 1.14)	**< 0.001**	**0.020**	**< 0.001**	**< 0.001**
LVEF	47.4 (40.2, 55.1)	50.8 (43.8, 57.1)	53.6 (47.5, 59.2)	**< 0.001**	**0.001**	**< 0.001**	**< 0.001**
LV GLS	− 13.2 (− 16.5, − 10.1)	− 17.4 (− 20.5, − 13.8)	− 19.1 (− 22.2, − 16.0)	**< 0.001**	**< 0.001**	**< 0.001**	**< 0.001**
LV GCS	− 20.8 (− 25.2, − 16.9)	− 25.0 (− 29.6, − 19.2)	− 26.6 (− 30.2, − 23.0)	**< 0.001**	**< 0.001**	**0.002**	**< 0.001**
LV GRS	18.2 (14.2, 22.6)	20.4 (14.8, 27.6)	22.9 (18.1, 27.5)	**< 0.001**	**< 0.001**	**0.004**	**< 0.001**
LA reservoir	20.2 (15.5, 25.3)	20.7 (15.2, 25.2)	21.7 (17.6, 26.3)	**0.004**	0.744	**0.024**	**0.001**
LA conduit	8.25 (4.79, 11.0)	8.40 (5.60, 11.5)	9.47 (6.44, 12.8)	**< 0.001**	0.381	**0.006**	**< 0.001**
LA booster	11.6 (8.81, 15.5)	11.3 (7.80, 15.4)	11.6 (8.76, 15.3)	0.677	0.729	0.405	0.538

Data presented as median (IQR) for the entire study collective. *p* values were calculated using the Mann–Whitney *U* test for the comparison of two infarct-related arteries and the Kruskal–Wallis test for the comparison of all three groups. *p* values in bold type indicate a significant difference. Functional parameters as well as area at risk, IS and MVO are reported in %

MS myocardial salvage, *MVO* microvascular obstruction, *LVEF* left ventricular ejection fraction, *LV GLS/GCS/GRS* left ventricular global longitudinal/circumferential/radial strain, *LA* left atrium

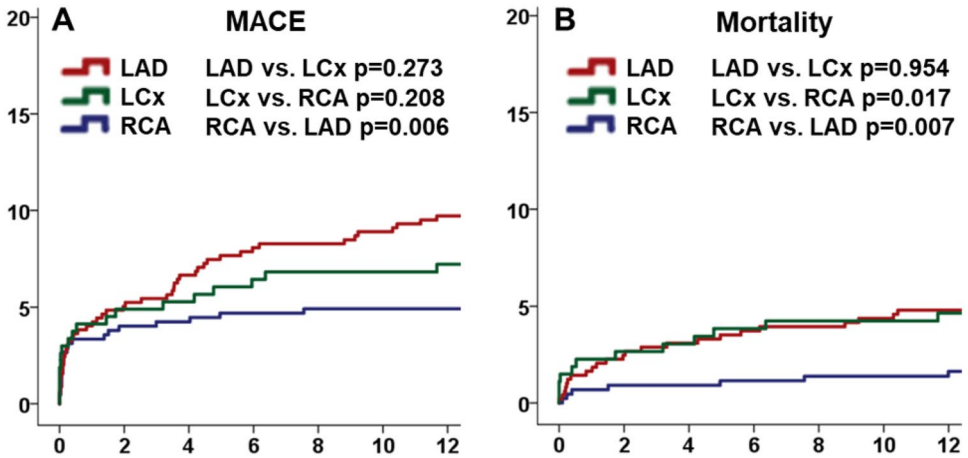

Fig. 3 IRA-associated risk for adverse events. The graph shows the different risk for **a** major adverse clinical events (MACE) occurrence or **b** mortality classified according to the infarct-related artery (IRA). Statistical analyses were performed using Log-rank test. *LAD* left anterior descending, *LCx* left circumflex artery, *RCA* right coronary artery

MACE occurrence are reported Table 3. LV tissue characterisation (IS and MVO) only differed between patients with and without MACE in LAD (IS $p=0.004$, MVO $p=0.046$), but not LCx or RCA lesions. The area at risk did not differ between MACE and no MACE for any IRA. Cardiac functional parameters differed between patients with and without MACE and were most severely impaired in LAD lesions with MACE ($p \leq 0.003$ for all) followed by LCx and RCA lesions. GLS and atrial reservoir function (ε_s) were the only parameters that differed significantly between patients with and without MACE amongst all IRA. Differences in tissue characterisation and cardiac function comparing patients with and without MACE were less pronounced in NSTEMI compared to STEMI patients (Supplement Tables S3 and S4).

Risk stratification

Univariate cox regression analyses are reported in Table 4. LV tissue characterisation did not allow for IRA-independent risk stratification. In addition to clinical Killip class scoring, cardiac functional parameters (LVEF, LV GLS and LA ε_s) were associated with MACE occurrence independent of IRA. Based on AUC analysis, εs (LAD, RCA) and GLS (LCx) best predicted MACE (AUC > 0.69). Multivariate cox regression models considered IRA-specific univariate significant baseline characteristics, ventricular (LVEF and GLS) as well as atrial function (ε_s) that demonstrated significance of cardiac functional parameters amongst all IRA (LVEF, GLS and ε_s). In LAD lesions, the number of diseased vessels (HR 1.75, 95%

Table 3 Cardiac performance-MACE

Parameter	Primary lesion								
	LAD			LCX			RCA		
	No mace ($n=450$)	Mace ($n=48$)	p	No mace ($n=249$)	Mace ($n=19$)	p	No mace ($n=426$)	Mace ($n=22$)	p
Area at risk	34.1 (24.4, 48.4)	39.5 (27.8, 57.1)	0.200	23.2 (18.1, 31.5)	25.0 (18.4, 33.5)	0.656	27.3 (18.4, 39.0)	36.1 (23.3, 42.6)	0.203
Infarct size	16.1 (6.15, 25.3)	24.4 (11.4, 34.4)	**0.004**	11.4 (5.10, 18.8)	15.8 (9.75, 28.7)	0.079	11.0 (5.00, 18.6)	17.3 (5.60, 22.4)	0.421
MS index	55.4 (33.5, 74.8)	41.8 (24.5, 58.5)	0.069	49.6 (30.0, 70.3)	23.4 (10.5, 55.5)	**0.031**	58.5 (39.1, 78.6)	64.2 (35.0, 80.6)	0.894
MVO	0.48 (0.00, 2.31)	1.65 (0.00, 5.19)	**0.046**	1.20 (0.00, 3.20)	1.38 (0.38, 5.59)	0.593	0.00 (0.00, 1.13)	0.00 (0.00, 1.52)	0.768
LVEF	47.9 (41.7, 55.5)	39.1 (32.2, 48.2)	**< 0.001**	51.1 (44.6, 57.1)	41.5 (32.1, 59.0)	0.077	53.8 (48.4, 59.2)	44.5 (38.0, 55.7)	**0.006**
LV GLS	− 13.5 (− 16.7, − 10.5)	− 10.7 (− 13.0, − 7.89)	**< 0.001**	− 17.4 (− 20.5, − 14.1)	− 9.41 (− 20.6, − 7.50)	**0.013**	− 19.2 (− 22.3, − 16.1)	− 16.6 (− 19.0, − 12.7)	**0.009**
LV GCS	− 21.0 (− 25.4, − 17.4)	− 17.2 (− 21.9, − 14.5)	**< 0.001**	− 25.7 (− 29.9, − 20.1)	− 15.7 (− 25.0, − 9.54)	**0.003**	− 26.7 (− 30.2, − 23.2)	− 21.0 (− 32.0, − 15.9)	0.116
LV GRS	18.5 (14.6, 22.8)	15.2 (11.4, 19.8)	**0.002**	20.5 (15.3, 27.8)	14.7 (9.82, 22.4)	**0.037**	23.1 (18.1, 27.6)	22.2 (16.4, 27.2)	0.503
LA reservoir	20.4 (16.2, 25.7)	14.7 (11.3, 20.4)	**< 0.001**	20.9 (15.8, 26.3)	17.8 (10.5, 22.0)	**0.048**	22.0 (17.9, 26.7)	17.4 (13.2, 22.2)	**0.004**
LA conduit	8.47 (5.27, 11.2)	4.55 (2.57, 8.80)	**< 0.001**	8.47 (5.44, 11.6)	8.28 (6.52, 8.90)	0.706	9.68 (6.60, 12.9)	6.50 (4.02, 8.71)	**0.003**
LA Booster	11.8 (8.98, 15.8)	10.0 (5.90, 12.3)	**0.003**	11.5 (8.19, 15.6)	6.77 (2.86, 12.4)	**0.004**	11.7 (8.82, 15.5)	10.8 (7.87, 13.6)	0.157

Data presented as median (IQR) for the entire study collective. p values were calculated using the Mann–Whitney U test for the comparison of patients with and without mace in each infarct-related artery. p values in bold type indicate a significant difference. Functional parameters as well as area at risk, IS and MVO are reported in %

MS myocardial salvage, *MVO* microvascular obstruction, *LVEF* left ventricular ejection fraction, *LV GLS/GCS/GRS* left ventricular global longitudinal/circumferential/radial strain, *LA* left atrium

Table 4 Risk for MACE

Variable	Univariate hazard ratio (CI) LAD	p	Univariate hazard ratio (CI) LCx	p	Univariate hazard ratio (CI) RCA	p
Infarct size	1.00 (1.00–1.01)	0.630	1.04 (1.00–1.09)	0.082	1.01 (0.97–1.06)	0.581
MVO	1.08 (1.01–1.15)	**0.032**	1.09 (0.96–1.23)	0.194	1.00 (0.77–1.30)	0.985
MS index	0.99 (0.98–1.00)	0.104	0.98 (0.95–1.00)	0.042	1.00 (0.98–1.02)	0.932
Number of diseased vessels	1.69 (1.20–2.39)	**0.003**	1.41 (0.79–2.50)	0.242	1.21 (0.73–2.01)	0.447
Killip class	1.83 (1.28–2.61)	**0.001**	2.25 (1.50–3.37)	**< 0.001**	2.02 (1.31–3.13)	**0.002**
TIMI flow pre	0.97 (0.76–1.24)	0.815	0.82 (0.56–1.22)	0.330	1.00 (0.71–1.42)	0.989
TIMI flow post	0.96 (0.61–1.53)	0.878	0.58 (0.35–0.97)	**0.039**	0.67 (0.39–1.15)	0.147
LVEF	0.93 (0.91–0.96)	**< 0.001**	0.95 (0.91–1.00)	**0.031**	0.94 (0.90–0.98)	**0.001**
LV GLS	1.14 (1.06–1.22)	**< 0.001**	1.17 (1.07–1.28)	**0.001**	1.12 (1.03–1.22)	**0.006**
LV GCS	1.09 (1.04–1.14)	**0.001**	1.12 (1.05–1.20)	**< 0.001**	1.05 (0.99–1.12)	0.124
LV GRS	0.93 (0.88–0.98)	**0.006**	0.92 (0.85–1.00)	**0.044**	0.99 (0.93–1.05)	0.723
LA reservoir strain	0.89 (0.85–0.94)	**< 0.001**	0.93 (0.86–1.00)	**0.038**	0.91 (0.85–0.97)	**0.005**
LA conduit strain	0.85 (0.78–0.92)	**< 0.001**	0.99 (0.88–1.13)	0.985	0.86 (0.77–0.97)	**0.010**
LA booster strain	0.89 (0.83–0.96)	**0.001**	0.84 (0.74–0.95)	**0.004**	0.93 (0.84–1.02)	0.111

Univariate cox regressions were performed in each subgroup of infarct-related artery separately. p values in bold type indicate a significant difference. Functional parameters as well as IS and MVO are reported in %

CI confidence interval, *MS* myocardial salvage, *MVO* microvascular obstruction, *TIMI* thrombolysis in myocardial infarction, *LVEF* left ventricular ejection fraction, *LV GLS/GCS/GRS* left ventricular global longitudinal/circumferential/radial strain, *LA* left atrium

CI 1.12–2.74, $p=0.014$) and atrial function εs (HR 0.92, 95% CI 0.86–0.99, $p=0.017$) were independently associated with MACE occurrence, in LCx lesions Killip class (HR 2.06, 95% CI 1.24–3.40, $p=0.005$) and ventricular function GLS (HR 1.12, 95% CI 1.01–1.25, $p=0.034$) and none in RCA lesions.

Discussion

The present study confirms increased mortality for LAD and LCx as compared to RCA lesions and reports IRA-specific underlying morphologic as well as functional differences following AMI. LV dysfunction was highest in LAD followed

by LCx and RCA lesions; similarly, LA function was impaired in either LAD or LCx compared to RCA lesions. GLS and εs were associated with outcome independent of IRA. Multivariate analyses revealed independent value beyond baseline confounders and LVEF for atrial strain (ε_s) in LAD and GLS in LCx lesions. These observations are likely to reflect underlying pathophysiology accounting for the observed differences in MACE rates and may have implications in disease management beyond risk stratification.

IRA-associated outcome and underlying pathophysiology

Discussions about IRA-associated prognosis are still ongoing; however, there is convincing evidence suggesting lower mortality in RCA lesions [10–15] which was confirmed by the present study. Cardiac functional analyses revealed IRA-dependent pathophysiological differences following AMI, which may explain these observations. LV dysfunction differed between all IRAs, being highest in LAD, followed by LCx and RCA lesions. The LV is mainly supplied by the LAD, with four [36] to eight [37] segments being exclusively subtended by the LAD. The LCx supplies parts of the lateral and the RCA parts of the posterior wall [36]. Importantly, the inferolateral region has the greatest overlap in myocardial perfusion, supplied by either RCA or LCx. Similarly, the inferoseptal region may be supplied by either of all three coronary arteries. There is evidence to suggest that RCA-supplied myocardium possesses most commonly high degrees of collateral blood supply [36]. Reduced blood flow in RCA and LCx lesions and their effect on cardiac mechanics may, therefore, be compensated by collaterals more easily, potentially limiting the impact of LCx and RCA lesions on LV function as opposed to LAD lesions. It is important to note that GLS but not LVEF, GCS, GRS or IS revealed differences between all IRA including STEMI and NSTEMI subgroups. GLS has shown superiority over LVEF in outcome prediction following myocardial infarction [19, 29] and may, thus, be the most sensitive parameter to detect subtle changes within myocardial contractility between different IRA as opposed to sheer IS. The reason for the superiority of GLS over simple assessments of myocardial damage (IS) may well lie in its ability to assess infarct and remote myocardial areas allowing a comprehensive quantification of LV function. In fact, impairment and diagnostic value of myocardial tissue beyond infarcted areas is confirmed by tissue characterisation by means of T1 mapping of remote myocardium showing incremental prognostic value over LVEF following STEMI [38] and in patients with coronary artery disease [39]. In the present study, IS was largest in LAD lesions thus also resulting in a large gray zone which is subject to microvascular dysfunction leading to adverse ventricular remodeling [40] and may explain in part why anterior AMI is prone to ventricular arrhythmia [41] which is further associated with mortality [42].

Alongside ventricular function, LA function and dilatation have proven independent prognostic value in addition to LVEF [43] including after MI [44, 45]. Interestingly, besides GLS, only εs was associated with outcome independent of IRA. Initially mainly attributed to be the result of LV dysfunction [46], novel data also provide evidence for impact of atrial infarction on dilatation and dysfunction [47]. In the present study population, LA function was equally impaired in both LAD and LCx but distinctly less in RCA lesions. The LA is most commonly supplied by a branch coming from the LCx [48]. Potentially, the extent of LA dysfunction may, thus, be first the result of ischemia in proximal LM and LCx lesions impacting the branch supplying the LA, and second the result of LV dysfunction in LAD lesions, both of which impact outcome.

The degree of transmurality is most commonly used for risk assessment following MI [49] but despite differences in LV tissue characterisation, such as largest IS in LAD or largest MVO in LCx-related infarction, tissue characterisation was not generally applicable for risk stratification as demonstrated by uni- and multivariate cox regression analyses in the present population.

Interestingly, IRA-dependent differences in prognosis seem to be reversed if patients go into cardiogenic shock (CS), with mortality being no longer dependent on IRA [14]. Although some existing studies report worsened outcome in LM lesions [7, 50] in CS patients, it is important to note that within these studies, TIMI flow post PCI was significantly lower in LM lesions and the rate of PCI remained undisclosed, both of which may represent major confounders in data interpretation. Noteworthy, in the present study, stent implantation was performed in 97.2% of all cases, and not differing between IRA with similar TIMI flow grades after PCI.

Risk stratification

Accounting for the tremendous variability of coronary artery distribution patterns [36, 37] and the clinical demand for standardized functional assessments, it is noteworthy that amongst all cardiac functional parameters, LV, GLS and LA εs were the most reliable parameters. First, they were the only parameters which were decreased in patients with MACE compared to patients without, independent of IRA. Second, given the fact that the degree of LV and LA dysfunction was distinctly lower in NSTEMI compared to STEMI patients, LV GLS (in LCx lesions) and LA εs (in LAD and RCA lesions) continuously discriminated patients with and without MACE both in STEMI and NSTEMI. The excellent diagnostic value of GLS is further confirmed in cox regression analyses for all IRA both in STEMI and

NSTEMI patients. AMI hits the endocardial myocardium first and may thus affect these regions more severely. Considering longitudinal fiber orientation is most pronounced in the endocardial region, GLS may indeed be the most global and precise parameter for risk evaluation independent of the culprit vessel [21, 29, 51]. In multivariate cox regression considering clinical parameters as well as ventricular and atrial function, atrial peak strain εs is independently associated with outcome in LAD lesions, whilst GLS is independently associated with outcome in LCx lesions. Considering coronary artery distribution patterns [37, 48], it is interesting to speculate about compensatory features of cardiac chambers with an impact beyond the lesion itself.

Patients with RCA lesions had the most preserved LV and LA function as compared to other IRA. Differences in cardiac function comparing patients with and without MACE were predominantly pronounced for LVEF, GLS and Es. Multivariate regression revealed neither of these parameters independent for risk assessment.

Limitations

In a multi-center setting, CMR scanning was conducted on different clinically established scanners from different vendors. Nevertheless, a standardized protocol was employed, and imaging results were evaluated in a blinded and experienced core-laboratory. Although the optimal timepoint for imaging following infarction is unknown, timepoints were similar for different culprit vessels, thus not influencing the comparison of these subgroups. Despite the detailed evaluation of IRA and resulting impaired LA and LV function, the study lacks data on the location of the culprit lesions within each vessel and on the supply pattern of coronary arteries. Furthermore, there is no information on ischemia in the remote territories in multi-vessel disease. On the one hand, unstable critically ill patients were not subjected to CMR imaging, which represents a selection bias. On the other hand, deformation imaging already enables reliable risk stratifications in this potentially lower risk collective. Whether it would achieve even higher diagnostic accuracy in the presence of more MACE remains speculative. Subgroup analyses result in lower numbers tested impacting statistical reliability. On the one hand, some parameters tested might lose significance; on the other hand, remaining significant parameters are likely to be very robust.

Conclusions

CMR allows for IRA-specific phenotyping and characterisation of morphologic and functional impairments following AMI. Quantitative mechanical (but not volumetric) atrial and ventricular alterations strongly depend on the culprit artery and provide pathophysiological correlates of observed differences in patient outcome. These observations may pave the way for novel diagnostic and therapeutic targets following AMI which need to be further investigated in future prospective trials.

Funding German Centre for Cardiovascular Research (DZHK).

References

1. Roffi M, Patrono C, Collet J-P, Mueller C, Valgimigli M, Andreotti F et al (2016) 2015 ESC Guidelines for the management of acute coronary syndromes in patients presenting without persistent ST-segment elevation: task force for the management of acute coronary syndromes in patients presenting without persistent ST-segment elevation of the european society of cardiology (ESC). Eur Heart J 37:267–315. https://doi.org/10.1093/eurheartj/ehv320
2. Smith SC, Collins A, Ferrari R, Holmes DR, Logstrup S, McGhie DV et al (2012) Our time: a call to save preventable death from cardiovascular disease (heart disease and stroke). Circulation 126:2769–2775. https://doi.org/10.1161/CIR.0b013e318267e99f
3. Reed GW, Rossi JE, Cannon CP (2017) Acute myocardial infarction. Lancet 389:197–210. https://doi.org/10.1016/S0140-6736(16)30677-8
4. Ali M, Lange SA, Wittlinger T, Lehnert G, Rigopoulos AG, Noutsias M (2017) In-hospital mortality after acute STEMI in patients undergoing primary PCI. Herz. https://doi.org/10.1007/s00059-017-4621-y
5. Dagres N, Hindricks G (2013) Risk stratification after myocardial infarction: is left ventricular ejection fraction enough to prevent sudden cardiac death? Eur Heart J 34:1964–1971. https://doi.org/10.1093/eurheartj/eht109
6. Stiermaier T, Jobs A, de Waha S, Fuernau G, Pöss J, Desch S et al (2017) Optimized prognosis assessment in ST-segment-elevation myocardial infarction using a cardiac magnetic resonance imaging risk score. Circ Cardiovasc Imaging. https://doi.org/10.1161/circimaging.117.006774
7. Trzeciak P, Gierlotka M, Gąsior M, Lekston A, Wilczek K, Słonka G et al (2013) Mortality of patients with ST-segment elevation myocardial infarction and cardiogenic shock treated by PCI is correlated to the infarct-related artery–results from the PL-ACS registry. Int J Cardiol 166:193–197. https://doi.org/10.1016/j.ijcard.2011.10.100
8. McDaniel MC, Galbraith EM, Jeroudi AM, Kashlan OR, Eshtehardi P, Suo J et al (2011) Localization of culprit lesions in coronary arteries of patients with ST-segment elevation myocardial infarctions: relation to bifurcations and curvatures. Am Heart J 161:508–515. https://doi.org/10.1016/j.ahj.2010.11.005
9. Velders MA, van Boven N, Boden H, van der Hoeven BL, Heestermans AACM, Jukema JW et al (2013) Association between angiographic culprit lesion and out-of-hospital cardiac arrest in ST-elevation myocardial infarction patients. Resuscitation 84:1530–1535. https://doi.org/10.1016/j.resuscitation.2013.07.016
10. Gho JMIH, Postema PG, Conijn M, Bruinsma N, de Jong JSSG, Bezzina CR et al (2017) Heart failure following STEMI: a contemporary cohort study of incidence and prognostic factors. Open Heart 4:e000551. https://doi.org/10.1136/openhrt-2016-000551
11. Stone PH, Raabe DS, Jaffe AS, Gustafson N, Muller JE, Turi ZG et al (1988) Prognostic significance of location and type of

myocardial infarction: independent adverse outcome associated with anterior location. J Am Coll Cardiol 11:453–463. https://doi.org/10.1016/0735-1097(88)91517-3
12. Hands ME, Lloyd BL, Robinson JS, de Klerk N, Thompson PL (1986) Prognostic significance of electrocardiographic site of infarction after correction for enzymatic size of infarction. Circulation 73:885–891. https://doi.org/10.1161/01.CIR.73.5.885
13. Kandzari DE, Tcheng JE, Gersh BJ, Cox DA, Stuckey T, Turco M et al (2006) Relationship between infarct artery location, epicardial flow, and myocardial perfusion after primary percutaneous revascularization in acute myocardial infarction. Am Heart J 151:1288–1295. https://doi.org/10.1016/j.ahj.2005.08.017
14. Fuernau G, Fengler K, Desch S, Eitel I, Neumann F-J, Olbrich H-G et al (2016) Culprit lesion location and outcome in patients with cardiogenic shock complicating myocardial infarction: a substudy of the IABP-SHOCK II-trial. Clin Res Cardiol 105:1030–1041. https://doi.org/10.1007/s00392-016-1017-6
15. Huey BL, Beller GA, Kaiser DL, Gibson RS (1988) A comprehensive analysis of myocardial infarction due to left circumflex artery occlusion: comparison with infarction due to right coronary artery and left anterior descending artery occlusion. J Am Coll Cardiol 12:1156–1166. https://doi.org/10.1016/0735-1097(88)92594-6
16. Schuster A, Morton G, Chiribiri A, Perera D, Vanoverschelde J-L, Nagel E (2012) Imaging in the management of ischemic cardiomyopathy: special focus on magnetic resonance. J Am Coll Cardiol 59:359–370. https://doi.org/10.1016/j.jacc.2011.08.076
17. Stiermaier T, Pöss J, Eitel C, de Waha S, Fuernau G, Desch S et al (2018) Impact of left ventricular hypertrophy on myocardial injury in patients with ST-segment elevation myocardial infarction. Clin Res Cardiol 107:1013–1020
18. Lønborg JT, Engstrøm T, Møller JE, Ahtarovski KA, Kelbæk H, Holmvang L et al (2013) Left atrial volume and function in patients following ST elevation myocardial infarction and the association with clinical outcome: a cardiovascular magnetic resonance study. Eur Heart J Cardiovasc Imaging 14:118–127. https://doi.org/10.1093/ehjci/jes118
19. Ersbøll M, Valeur N, Mogensen UM, Andersen MJ, Møller JE, Velazquez EJ et al (2013) Prediction of all-cause mortality and heart failure admissions from global left ventricular longitudinal strain in patients with acute myocardial infarction and preserved left ventricular ejection fraction. J Am Coll Cardiol 61:2365–2373. https://doi.org/10.1016/j.jacc.2013.02.061
20. Kühl JT, Møller JE, Kristensen TS, Kelbæk H, Kofoed KF (2011) Left atrial function and mortality in patients with NSTEMI an MDCT study. JACC Cardiovasc Imaging 4:1080–1087. https://doi.org/10.1016/j.jcmg.2011.08.008
21. Stillman AE, Oudkerk M, Bluemke DA, de Boer MJ, Bremerich J, Garcia EV et al (2018) Imaging the myocardial ischemic cascade. Int J Cardiovasc Imaging 34:1249–1263. https://doi.org/10.1007/s10554-018-1330-4
22. Thiele H, Wöhrle J, Hambrecht R, Rittger H, Birkemeyer R, Lauer B et al (2012) Intracoronary versus intravenous bolus abciximab during primary percutaneous coronary intervention in patients with acute ST-elevation myocardial infarction: a randomised trial. Lancet 379:923–931. https://doi.org/10.1016/S0140-6736(11)61872-2
23. Thiele H, de Waha S, Zeymer U, Desch S, Scheller B, Lauer B et al (2014) Effect of aspiration thrombectomy on microvascular obstruction in NSTEMI patients: the TATORT-NSTEMI trial. J Am Coll Cardiol 64:1117–1124. https://doi.org/10.1016/j.jacc.2014.05.064
24. Eitel I, Wöhrle J, Suenkel H, Meissner J, Kerber S, Lauer B et al (2013) Intracoronary compared with intravenous bolus abciximab application during primary percutaneous coronary intervention in ST-segment elevation myocardial infarction: cardiac magnetic resonance substudy of the AIDA STEMI trial. J Am Coll Cardiol 61:1447–1454. https://doi.org/10.1016/j.jacc.2013.01.048
25. Eitel I, de Waha S, Wöhrle J, Fuernau G, Lurz P, Pauschinger M et al (2014) Comprehensive prognosis assessment by CMR imaging after ST-segment elevation myocardial infarction. J Am Coll Cardiol 64:1217–1226. https://doi.org/10.1016/j.jacc.2014.06.1194
26. Schuster A, Stahnke V-C, Unterberg-Buchwald C, Kowallick JT, Lamata P, Steinmetz M et al (2015) Cardiovascular magnetic resonance feature-tracking assessment of myocardial mechanics: intervendor agreement and considerations regarding reproducibility. Clin Radiol 70:989–998. https://doi.org/10.1016/j.crad.2015.05.006
27. Backhaus SJ, Stiermaier T, Lange T, Chiribiri A, Lamata P, Uhlig J et al (2018) Temporal changes within mechanical dyssynchrony and rotational mechanics in Takotsubo syndrome: a cardiovascular magnetic resonance imaging study. Int J Cardiol 273:256–262. https://doi.org/10.1016/j.ijcard.2018.04.088
28. Kowallick JT, Kutty S, Edelmann F, Chiribiri A, Villa A, Steinmetz M et al (2014) Quantification of left atrial strain and strain rate using cardiovascular magnetic resonance myocardial feature tracking: a feasibility study. J Cardiovasc Magn Reson 16:60. https://doi.org/10.1186/s12968-014-0060-6
29. Eitel I, Stiermaier T, Lange T, Rommel KP, Koschalka A, Kowallick JT et al (2018) Cardiac magnetic resonance myocardial feature tracking for optimized prediction of cardiovascular events following myocardial infarction. JACC Cardiovasc Imaging 11:1433–1444. https://doi.org/10.1016/j.jcmg.2017.11.034
30. Backhaus SJ, Schuster A (2018) Atrial strain assessment in left ventricular diastolic dysfunction. JACC Cardiovasc Imaging 11:154. https://doi.org/10.1016/j.jcmg.2017.10.016
31. Kowallick JT, Morton G, Lamata P, Jogiya R, Kutty S, Hasenfuß G et al (2015) Quantification of atrial dynamics using cardiovascular magnetic resonance: inter-study reproducibility. J Cardiovasc Magn Reson 17:36. https://doi.org/10.1186/s12968-015-0140-2
32. Morton G, Schuster A, Jogiya R, Kutty S, Beerbaum P, Nagel E (2012) Inter-study reproducibility of cardiovascular magnetic resonance myocardial feature tracking. J Cardiovasc Magn Reson 14:43. https://doi.org/10.1186/1532-429X-14-43
33. Kowallick JT, Silva Vieira M, Kutty S, Lotz J, Hasenfuß G, Chiribiri A, Schuster A (2017) Left atrial performance in the course of hypertrophic cardiomyopathy: relation to left ventricular hypertrophy and fibrosis. Invest Radiol 52:177–185. https://doi.org/10.1097/RLI.0000000000000326
34. Schuster A, Hor KN, Kowallick JT, Beerbaum P, Kutty S (2016) Cardiovascular magnetic resonance myocardial feature tracking: concepts and clinical applications. Circ Cardiovasc Imaging 9:e004077. https://doi.org/10.1161/circimaging.115.004077
35. Gertz RJ, Lange T, Kowallick JT, Backhaus SJ, Steinmetz M, Staab W et al (2018) Inter-vendor reproducibility of left and right ventricular cardiovascular magnetic resonance myocardial feature-tracking. PLoS One 13:e0193746
36. Ortiz-Pérez JT, Rodríguez J, Meyers SN, Lee DC, Davidson C, Wu E (2008) Correspondence between the 17-segment model and coronary arterial anatomy using contrast-enhanced cardiac magnetic resonance imaging. JACC Cardiovasc Imaging 1:282–293. https://doi.org/10.1016/j.jcmg.2008.01.014
37. Pereztol-Valdés O, Candell-Riera J, Santana-Boado C, Angel J, Aguadé-Bruix S, Castell-Conesa J et al (2005) Correspondence between left ventricular 17 myocardial segments and coronary arteries. Eur Heart J 26:2637–2643. https://doi.org/10.1093/eurheartj/ehi496
38. Reinstadler SJ, Stiermaier T, Liebetrau J, Fuernau G, Eitel C, de Waha S et al (2018) Prognostic significance of remote myocardium alterations assessed by quantitative noncontrast T1 mapping

in ST-segment elevation myocardial infarction. JACC Cardiovasc Imaging 11:411–419. https://doi.org/10.1016/j.jcmg.2017.03.015
39. Puntmann VO, Carr-White G, Jabbour A, Yu C-Y, Gebker R, Kelle S et al (2018) Native T1 and ECV of noninfarcted myocardium and outcome in patients with coronary artery disease. J Am Coll Cardiol 71:766–778. https://doi.org/10.1016/j.jacc.2017.12.020
40. Cheng R, Wei G, Yu L, Su Z, Wei L, Bai X et al (2014) Coronary flow reserve in the remote myocardium predicts left ventricular remodeling following acute myocardial infarction. Yonsei Med J 55:904–911. https://doi.org/10.3349/ymj.2014.55.4.904
41. van der Weg K, Kuijt WJ, Tijssen JGP, Bekkers SCAM, Haeck JDE, Green CL et al (2015) Prospective evaluation of where reperfusion ventricular arrhythmia "bursts" fit into optimal reperfusion in STEMI. Int J Cardiol 195:136–142. https://doi.org/10.1016/j.ijcard.2015.05.106
42. Mehta RH, Starr AZ, Lopes RD, Hochman JS, Widimsky P, Pieper KS et al (2009) Incidence of and outcomes associated with ventricular tachycardia or fibrillation in patients undergoing primary percutaneous coronary intervention. JAMA 301:1779–1789. https://doi.org/10.1001/jama.2009.600
43. Backhaus SJ, Stiermaier T, Lange T, Chiribiri A, Uhlig J, Freund A, et al. Atrial mechanics and their prognostic impact in Takotsubo syndrome: a cardiovascular magnetic resonance imaging study. Eur Heart J Cardiovasc Imaging. **(In press)**
44. Moller JE, Hillis GS, Oh JK, Seward JB, Reeder GS, Wright RS et al (2003) Left atrial volume: a powerful predictor of survival after acute myocardial infarction. Circulation 107:2207–2212. https://doi.org/10.1161/01.CIR.0000066318.21784.43
45. Schuster A, Backhaus SJ, Stiermaier T, Navarra JL, Uhlig J, Rommel KP et al (2018) P3695 quantitative left atrial function allows optimized prediction of cardiovascular events following myocardial infarction: a cardiovascular magnetic resonance imaging study. Eur Heart J. https://doi.org/10.1093/eurheartj/ehy563.p3695
46. Møller JE, Pellikka PA, Hillis GS, Oh JK (2006) Prognostic importance of diastolic function and filling pressure in patients with acute myocardial infarction. Circulation 114:438–444. https://doi.org/10.1161/circulationaha.105.601005
47. Aguero J, Galan-Arriola C, Fernandez-Jimenez R, Sanchez-Gonzalez J, Ajmone N, Delgado V et al (2017) Atrial infarction and ischemic mitral regurgitation contribute to post-MI remodeling of the left atrium. J Am Coll Cardiol 70:2878–2889. https://doi.org/10.1016/j.jacc.2017.10.013
48. Boppana VS, Castaño A, Avula UMR, Yamazaki M, Kalifa J (2011) Atrial coronary arteries: anatomy and atrial perfusion territories. J Atr Fibrillation 4:375. https://doi.org/10.4022/jafib.375
49. Choi KM, Kim RJ, Gubernikoff G, Vargas JD, Parker M, Judd RM (2001) Transmural extent of acute myocardial infarction predicts long-term improvement in contractile function. Circulation 104:1101–1107. https://doi.org/10.1161/hc3501.096798
50. Kunadian V, Qiu W, Ludman P, Redwood S, Curzen N, Stables R et al (2014) Outcomes in patients with cardiogenic shock following percutaneous coronary intervention in the contemporary era: an analysis from the BCIS database (british cardiovascular intervention society). JACC Cardiovasc Interv 7:1374–1385. https://doi.org/10.1016/j.jcin.2014.06.017
51. Greenbaum RA, Ho SY, Gibson DG, Becker AE, Anderson RH (1981) Left ventricular fibre architecture in man. Heart 45:248–263. https://doi.org/10.1136/hrt.45.3.248